AD-A163 694 NON-DESTRUCTIVE LASER HOLOGRAPHIC TESTING OF SOLID PROPELLANT FOR UNBONDING DEFECTS(U) FOREIGN TECHNOLOGY DIV WRIGHT-PATTERSON AFB OH Y WANG 15 JAN 86 1/1

UNCLASSIFIED FTD-ID(RS)T-0964-85 F/G 21/8.2 NL

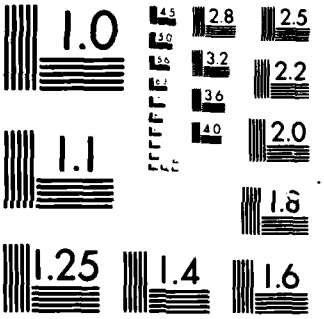

MICROCOPY RESOLUTION TEST CHART
NATIONAL BUREAU OF STANDARDS 1963-A

FTD-ID(RS)T-0964-85

AD-A163 694

FOREIGN TECHNOLOGY DIVISION

NON-DESTRUCTIVE LASER HOLOGRAPHIC TESTING OF SOLID PROPELLANT FOR UNBONDING DEFECTS

by

Wang Yongbao

DTIC
ELECTE
FEB 7 1986
S D
B

DTIC FILE COPY

Approved for public release;
distribution unlimited.

86 2 7 014

EDITED TRANSLATION

FTD-ID(RS)T-0964-85 15 Jan 86

MICROFICHE NR: FTD-86-C-001377

NON-DESTRUCTIVE LASER HOLOGRAPHIC TESTING OF SOLID PROPELLANT FOR UNBONDING DEFECTS

By: Wang Yongbao

English pages: 14

Source: Wusun Jiance, Vol. 6, Nr. 1, February 1984, pp. 4-7

Country of origin: China
Translated by: SCITRAN
F33657-84-D-0165
Requester: FTD/TQTA
Approved for public release; distribution unlimited.

THIS TRANSLATION IS A RENDITION OF THE ORIGINAL FOREIGN TEXT WITHOUT ANY ANALYTICAL OR EDITORIAL COMMENT. STATEMENTS OR THEORIES ADVOCATED OR IMPLIED ARE THOSE OF THE SOURCE AND DO NOT NECESSARILY REFLECT THE POSITION OR OPINION OF THE FOREIGN TECHNOLOGY DIVISION.

PREPARED BY:

TRANSLATION DIVISION
FOREIGN TECHNOLOGY DIVISION
WP-AFB, OHIO.

GRAPHICS DISCLAIMER

All figures, graphics, tables, equations, etc. merged into this translation were extracted from the best quality copy available.

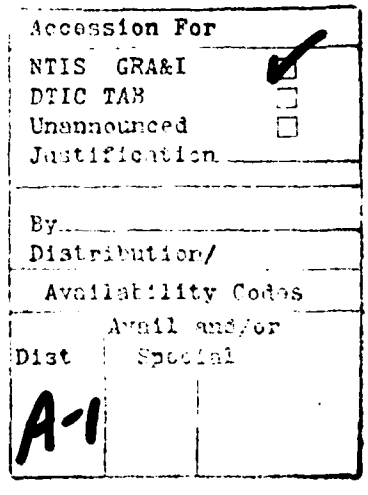

Non-destructive Laser Holographic Testing of Solid Propellant /4 for Unbonding Defects

Northwestern Polytechnical University, Wang Yongbao

This paper describes the feasibility and sensitivity of using a laser holographic technique to detect unbonding defects in solid propellant rocket components.

Introduction

The solid rocket engine is comprised of an external shell, an insulating layer, a coating and the propellant. The external shell is a metallic (steel or aluminum alloy) or fiber glass cylinder. The insulating layer, the coating and the propellant column are made of rubber or plastic materials with some elasticity. The technical requirement is that there should be no unbonding defects between the interface. Otherwise, a "serial firing" phenomenon will occur, which not only will affect the performance of the engine but also will lead to rocket engine explosion in serious cases. X-ray pictures can be used to discover defects such as bubbles and impurities in the propellant. Unbonding defects, however, are difficult to uncover. Ultrasound or acoustic resistance tests are limited because a coupling agent is required at the probe (composite propellants are not allowed to come in contact with solvents). In addition, certain portions of the engine with large curvature and edge angle cannot be approached by probes due to structural and dimensional limitations. Therefore, an ideal and reliable

test method has not yet been found to date. First, we collaborated with relevant organizations. They provided specimens with artificially made unbonding defects. We first used the non-destructive laser holographic testing method to examine a segment of the specimen. Then, we conducted tests on flat plate specimens with artificially made unbonding defects. Based on the experimental results, the non-destructive laser holographic testing is effective in detecting unbonding damages in a solid propellant engine. It is worth further investigation. In order to determine the sensitivity of this non-destructive testing method, propellant, coating and shell materials (composite materials) are used as specimens to systematically perform sensitivity tests. The detectable debonding area (expressed in terms of its diameter) to defect depth ratio is obtained. This paper describes the detection method, experimental apparatus and results.

Experimental Method and Apparatus

1. Experimental Method

Laser holographic techniques include the real time method, double exposure method and time averaging method. The double exposure method was chosen for this experiment after considering the facts that the equipment required is simple, it is convenient to operate, the intensity of the interference fringe pattern can be easily enhanced, the clarity of the hologram is high and the results can be saved over a long period of time.

2. Shock-proof Platform

Laser holography utilizes the principle of interference

between the light from an object and a reference light to record the amplitude and phase information of the object light. Thus, it is required that the relative displacement of the two light beams should not exceed one eighth of the wavelength in the recording process. Otherwise, the interference pattern will be mixed up to create a blurred image. It may even totally disappear. Hence, it is necessary to use a shock proof platform to maintain the relative stability of the holographic system. The platform used is a 1.4 x 3m cast iron platform which weighs 3 tons. The two ends of the platform are supported by cement blocks. The bottom of the cement block is filled with many layers of foam rubber and sand to absorb the external vibration transmitted through the ground.

3. Layout of the Optical Path

In this experiment, a tuneable internal cavity He-Ne laser was used as the light source. The single mode power output is 39mW. The optical path layout is shown in Figure 1.

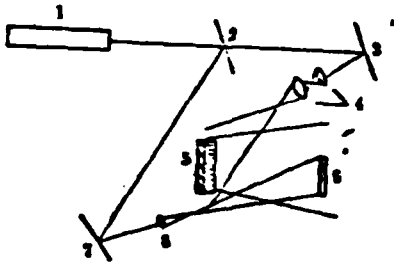

Figure 1. The Optical System

The laser beam is emitted from a He-Ne laser. The beam is split into two by the beam splitter 2. One light beam which passes through the beam splitter 2, is reflected by the mirror 3 and illuminates the specimen 5 through the lens 4. It is scattered by the specimen and reflected to the holographic interference plate 6. The other beam is reflected by the beam splitter 2 and then shines directly on the holographic interference plate through the mirror 7 and lens 8. The optical path is approximately 2 m in either case. The angle between them is 30°. Their light intensity ratio is 1:2 ~ 1:6.

When the holographic interference plate was assembled, we waited 1 minute to allow the entire photographic system to stabilize before the shutter was opened for the 1st exposure. Then, the specimen was put on load. Because there is a lagging effect due to the deformation of the specimen, therefore, it is necessary to wait 1-2 minutes to proceed with the 2nd exposure. Sometimes, in order to shorten the exposure time, the interference plate could be sensitized (soaking the plate in 5% triethanolamine solution for several seconds)when the resolution of the holographic plate permits. When the light intensities were measured, 2CR62 silicon photocells were used to receive the light at the plate. It was displayed by a model AC15/1 dc ammeter.

4. Loading Method

A negative pressure load is primarily used in this experiment. The specimen is placed in a vacuum chamber made of plexiglass. A vacuum pump is used to pull a load on the

specimen. In order to stabilize the photographic system, the vacuum chamber is usually already in a high degree of vacuum. The vacuum is lowered to generate a suitable pressure difference between the surface and the unbonded site of the specimen to deform the specimen surface. The pressure differences at the first and second exposures are expressed in mmHg. In order to ascertain the magnitude of the load, a real time method was /5 used to determine the appropriate load prior to recording the data by the double exposure method.

5. The exposed interference plates are developed and fixed by wet chemicals to become holograms. They are bleached to improve the scattering efficiency. They are then soaked in 50%, 75% and 90% ethanol solutions for 1 minute each on order to accelerate the drying process of the negative and improve the clarity.

Experimental Results

1. Figure 2 shows a simulated specimen of a solid propellant. Load is applied by heating. The annular pattern shown on the upper left corner of the interference pattern obtained by the double exposure method shows the artificially made unbonding defect between the aluminum alloy cylinder and the insulating layer.

Figure 2

2. The structure and dimensions of the specimen plate used to detect artificial unbonding defects are shown in Figure 3. The positions and sizes of artificially made unbonding sites (by placing paper circles soaked with a release agent) are shown in Table1.

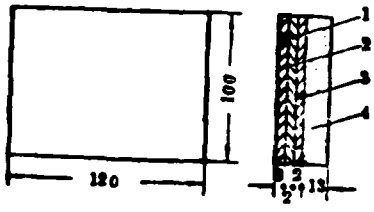

Figure 3

Table 1 Positions and Sizes of Defects

1. 试件号	2. 脱粘深度	3 缺陷部位及尺寸(毫米)			
		4 左上角	5 左下角	6 右上角	7 右下角
1	绝热层与包复层界面之间	φ12	φ5	φ8	φ3
2	包复层与火药柱界面之间	φ12	φ5	φ8	φ3

1. specimen number
2. depth of unbonding
3. defect position and size (mm)
4. upper left corner
5. lower left corner
6. upper right corner
7. lower right corner
8. between the insulating layer and the coating
9. between the coating and the propellant

Figure 4 shows the interference pattern of specimen 1 under a negative load at 164 mmHg pressure difference between two exposures. There are four defects in the upper part. On the lower left corner, there is a unbonding defect with a 5 mm diameter at the turning point of the interference pattern. The 3 mm diameter unbonding defect 17mm deep from the surface of the propellant on the lower right corner was not detected.

Figure 4

Figure 5 shows the interference pattern of specimen 2 at a pressure difference of 160 mmHg. The fringes are concentrated at the top, indicating that enclosed ring pattern shows an unbonding defect. The turn at the lower left corner is a 5 mm diameter unbonding defect. The lower right fringe slightly turns, showing that there is a 3 mm diameter unbonding defect 15 mm deep into the propellant surface.

Figure 5

3. Sensitivity of the detection test. The use of laser holography to detect the internal defects of an object is realized by applying a load to create a small deformation corresponding to the defects. When this deformation reaches one quarter of the laser wavelength used, the interference pattern may reflect these defects. When an He-Ne laser is used as the light source, it is possible to detect a 0.2 micron deformation with the aid of laser holography. If defects are located near the surface, it is very easy to create the deformation mentioned above by applying a non-destructive load. When the defects are located very deep, it is more difficult to show a 0.2 micron deformation on the surface of the object. In this case, only larger defects can be displayed. In other words, the sensitivity of detection is determined by the depth to defect area ratio.

Table 2 shows the relation between the depth H and the /6
unbonding circle area (expressed in diameter d) ratio of a propellant column under a negative load.

Table 2

1. 试件号	缺陷尺寸 (以直径d表示,毫米)	缺陷深度 (H,毫米)	加载量 (毫米·汞柱)	H/d
1	0.965	2.80	234	2.90
2	2.080	6.05	234	2.908
3	3.093	8.75	164	2.828
4	4.067	11.59	188	2.849
5	4.974	14.14	231	2.842
6	6.550	19.31	234	2.948
7	6.909	19.78	231	2.862
8	8.164	23.50	457	2.878
9	9.049	26.21	234	2.895
10	10.173	30.05	86	2.944
11	11.047	32.43	74	2.935

1. specimen number
2. defect size (expressed in diameter d, mm)
3. defect depth (H, mm)
4. load (mmHg)

From the table we can see that the depth of the defect in specimen is very shallow, H=2.80. Therefore, very small unbonding defects (approximately 1 mm in diameter) could also be detected (see Figure 6). When the defects are deep (specimen 11, H=32.43), only larger defects (d=11.047) could be detected (see Figure 7).

Figure 6

Figure 7

As for specimen 6 (d=6.55). if the defect depth is 20 mm, when H/d reaches 3.053, any unbonding defect cannot be detected even by increasing the load (see Figure 8). When the defect depth is 19.31, however, it could be detected (see Figure 9). Based on these data, we can deduce that this detection method can resolve a 0.69 mm depth when the diameter of the unbonding defect on the propellant is 6.55 mm.

Based on Table 2 we can see that the H/d value is around 2.9. Different types of materials, however, have a different H/d value. The sensitivity of detection is also related to the

elastic modulus of the material. Table 3 list the H/d values of the coating of a specific product. Due to its larger modulus of elasticity, the value of H/d is approximately 0.7.

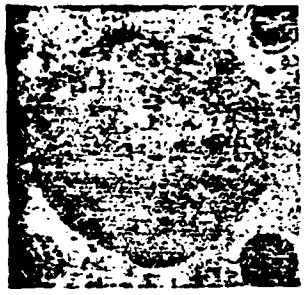

Figure 8

Figure 9

Table 3

1. 试件号	2. 缺陷大小(以直径d表示，毫米)	3. 缺陷深度(H，毫米)	H/d
1	2.59	1.875	0.724
2	3.94	2.77	0.703
3	7.165	4.885	0.682
4	10.146	7.315	0.721
5	13.197	9.30	0.705

1. specimen number
2. defect size (expressed in diameter d, mm)
3. defect depth (H, mm)

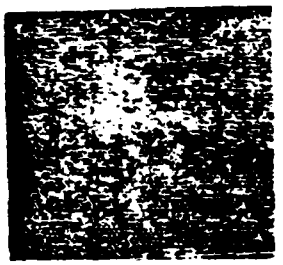

Figure 10

Figure 10 is the unbonding defect interference pattern of specimen 1 when the load applied is 44 mmHg. The defects are clearly displayed. When the load is increased, the interference /7 fringes also increase. They become denser. The location of the unbonding location, however, remains unchanged.

In addition, the sensitivity of detection is also directly related to the nature of the defect. For instance, the gas content at the unbonding defect can directly affect the

sensitivity of detection. The higher the gas content is, the higher the sensitivity of detection becomes. As for a composite material used for the external shell, when the defect site contains more gas (i.e., separation), its H/d value is 0.2. As for an unseparated defect (i.e., the so-called mechanical bonding), its H/d value is 0.08. The difference is substantial.

Conclusions

1. Laser holography can detect the unbonding defects between the propellant, coating, insulating layer and shell (Figures 4 and 5). X-ray could not detect such defects in similar specimens.

2. The sensitivity of detection depends on the H/d ratio. The ratio is around 2.9 for the propellant. When the H/d ratio is equal to or less than this value, even 1 mm diameter unbonding defects can be detected.

3. The value of H/d is related to the nature of the material (modulus of elasticity). The H/d value of the coat is around 0.7.

4. The sensitivity of detection also depends on the gas content at the defect. The sensitivity of detecting an unseparated defect is decreased by more than one half of that of detecting a separated defect.

END

FILMED

3-86

DTIC